



ELSEVIER

Physics Letters B 537 (2002) 62–68

PHYSICS LETTERS B

www.elsevier.com/locate/npe

Ground state properties of many-body systems in the two-body random ensemble and random matrix theory

L.F. Santos^a, Dimitri Kusnezov^a, Ph. Jacquod^b

^a Center for Theoretical Physics, Sloane Physics Lab, Yale University, New Haven, CT 06520-8120, USA

^b Instituut-Lorentz, Universiteit Leiden, PO Box 9506, 2300 RA Leiden, The Netherlands

Received 22 January 2002; received in revised form 18 April 2002; accepted 29 April 2002

Editor: W. Haxton

Abstract

We explore generic ground-state and low-energy statistical properties of many-body bosonic and fermionic one- and two-body random ensembles (TBRE) in the dense limit, and contrast them with random matrix theory (RMT). Weak differences in distribution tails can be attributed to the regularity or chaoticity of the corresponding Hamiltonians rather than the particle statistics. We finally show the universality of the distribution of the angular momentum gap between the lowest energy levels in consecutive J -sectors for the four models considered. © 2002 Elsevier Science B.V. All rights reserved.

PACS: 05.30.-d; 47.52.+j; 21.60.-n; 21.10.Re; 75.75.+a

Wigner introduced the Gaussian orthogonal ensemble (GOE) to deal with the statistics of high-lying levels of many-body quantum systems [1]. Although the fluctuations of certain observables predicted by the GOE agree well with experimental observations, it represents a system in which all the particles interact simultaneously and this is a priori not appropriate to describe many-body systems in which the two-body interaction is predominant [2,3]. The two-body random ensemble (TBRE) was introduced to improve upon the physical limitations of RMT [4]. The TBRE Hamiltonian includes only up to two-body operators, whose coefficients are real random numbers. This en-

semble reproduces a Gaussian level density and the GOE level repulsion as desired, but until recently, only the *dilute limit* was analytically tractable [5]. This limit corresponds to having a large number of particles ($N_p \gg 1$) and an even larger number of single-particle states $K \gg 1$, so that $N_p/K \ll 1$. In such a limit Pauli's principle has only a marginal effect, so particles statistics are unimportant. Many physical regimes lie outside the dilute limit: for bosonic particles, we may consider a large number of particles with a finite $K \ll N_p$; similarly, fermionic antisymmetry becomes relevant as one approaches half-filling, $N_p \approx K/2$. Since we are interested in those aspects, we do not restrict ourselves to the dilute limit. It has only recently been shown, from the connection between the Lanczos tridiagonalization and random polynomials, that this case can also be treated analytically in some instances [6].

E-mail addresses: santos@nst4.physics.yale.edu

(L.F. Santos), dimitri@mirage.physics.yale.edu (D. Kusnezov), pjacquod@lorentz.leidenuniv.nl (Ph. Jacquod).

We investigate the statistical properties of the low-lying levels of interacting complex systems, extracting from the edge of the spectra, generic properties that would reflect the basic structure of many-body systems such as molecules, atomic nuclei or quantum dots close to, or in their ground-state. We compute the lowest eigenvalue distribution for two bosonic and two fermionic TBREs and show that, after a proper rescaling, the distributions have a surprisingly weak dependence on the nature of the particles. Comparing to predictions from RMT lead to surprising similarities. The fact that the distribution of the lowest energy state depends only weakly on the nature of the particles and not on the ensemble used to study it points to its universality, but a closer inspection of the tails of these distributions indicate that they depend on the chaoticity of the system analyzed. To understand the role of chaos, we study models which are regular as well as chaotic and find that the tails of the ground state distributions for chaotic systems are closer to that obtained from the large- N GOE, while for integrable systems it is closer to the $N = 2$ GOE. The distribution of energy differences between the lowest energy levels in two consecutive angular momentum sector (J and $J + 1$) is found to be more robust, having the same shape in all four cases within numerical accuracy (deviations occur for the single j -shell model at small gap values). Since this distribution depends on correlations between Hilbert subspaces with different quantum numbers, it is outside the scope of RMT. We expect that this distribution is generic, a conclusion which is borne out by the bosonic nature of the corresponding excitation. Our analysis is based on numerical and analytical results. The analytical treatment is now possible not only for the TBRE [6], as already pointed out, but also for the large N limit of the GOE, for which an expression for the distribution function of the largest eigenvalue was obtained in terms of a particular Painlevé II function [7].

We start by summarizing analytical results obtained for the GOE. A general matrix H of this ensemble can be expressed in terms of a rotation matrix O and the diagonal eigenvalue matrix $E = \text{diag}(E_1, E_2, \dots, E_N)$ as $H = O^T E O$. The distribution of the ground state energy is $P(E_{\text{gs}}) = \langle \delta(E_{\text{gs}} - E_1) \rangle$, where $\langle \dots \rangle$ indicates GOE averaging and the

probability of having a matrix element H_{ij} is

$$P(H_{ij}) \propto \exp\left(-\frac{1}{2} \text{Tr} H^2\right).$$

Two limits are considered: $N = 2$ and $N \rightarrow \infty$. For $N = 2$, direct integration gives

$$\begin{aligned} P_2^{\text{GOE}}(E_{\text{gs}}) &= \frac{1}{2\sqrt{\pi}} \left\{ \exp(-E_{\text{gs}}^2) \right. \\ &\quad \left. - \sqrt{\frac{\pi}{2}} \exp(-E_{\text{gs}}^2/2) E_0 \left[\text{erfc}\left(\frac{E_{\text{gs}}}{\sqrt{2}}\right) \right] \right\}. \end{aligned} \quad (1)$$

This distribution is not readily calculated for arbitrary N , however, in the limit $N \rightarrow \infty$, Tracy and Widom [7] derived an expression for the distribution of the largest eigenvalue ($f_1(s)$ [7]), which in terms of the lowest eigenvalue is written as

$$\begin{aligned} P_\infty^{\text{GOE}}(E_{\text{gs}}) &= \frac{1}{2} \left(\int_{-E_{\text{gs}}}^{\infty} q(x)^2 dx + q(-E_{\text{gs}}) \right) \\ &\quad \times \exp \left[-\frac{1}{2} \left(\int_{-E_{\text{gs}}}^{\infty} (x + E_{\text{gs}}) q(x)^2 dx \right. \right. \\ &\quad \left. \left. + \int_{-E_{\text{gs}}}^{\infty} q(x) dx \right) \right]. \end{aligned} \quad (2)$$

Here $q(E_{\text{gs}})$ satisfies the Painlevé II equation and the boundary condition is $q(E_{\text{gs}}) \sim \text{Ai}(E_{\text{gs}})$ as $E_{\text{gs}} \rightarrow \infty$, where Ai is the Airy function. The numerical solutions for this expression are plotted on the top panel of Fig. 1, where one sees that it agrees well with the distribution for a GOE of $N = 200$. This function has the asymptotics

$$\begin{aligned} \log P_\infty^{\text{GOE}}(E_{\text{gs}}) &\sim -|E_{\text{gs}}|^3, \quad E_{\text{gs}} \rightarrow -\infty, \\ \log P_\infty^{\text{GOE}}(E_{\text{gs}}) &\sim -E_{\text{gs}}^{3/2}, \quad E_{\text{gs}} \rightarrow \infty. \end{aligned} \quad (3)$$

In contrast to $N = 2$, the tails deviate from Gaussian behavior. For completeness, we also show the average ground state energy for the GOE, although this quantity is not expected to have physical consequences. We find that

$$\langle E_{\text{gs}} \rangle = 2.01(2)\sqrt{N} + 1.58(2)N^{-1/6},$$

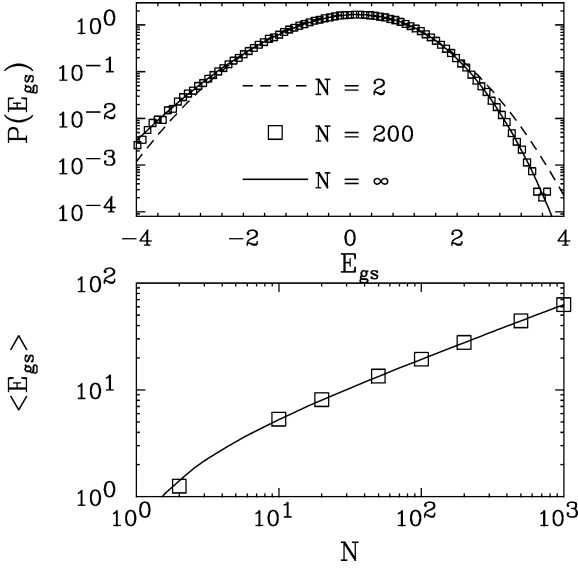


Fig. 1. Top: analytical distribution of the ground state energy for GOE of dimension $N = 2$ (dashed) and $N = \infty$ (solid). The numerically obtained distribution for $N = 200$ (squares) already coincides with the $N = \infty$ GOE. Bottom: average GOE ground-state energy $\langle E_{gs} \rangle$ as a function of the matrix size N . The solid line gives the theoretical estimate.

which agrees with the predicted functional form [7, 8]. On the bottom panel of Fig. 1, we show that this expression fits numerical results for $N \in [2, 1000]$.

In contrast to the GOE, the TBRE is not a purely statistical model, but rather is constructed in a particular bosonic or fermionic space. We take it in the form

$$H = \sum_{ij} \epsilon_{ij} a_i^+ a_j + \sum_{ijkl} V_{ijkl} a_i^+ a_j^+ a_k a_l. \quad (4)$$

When originally introduced, the Hamiltonian operators of the TBRE had only (interaction) two-body terms, but we include the one-body term. a_i^+ (a_i) represents boson or fermion creation (annihilation) operator and the coefficients ϵ_{ij} and V_{ijkl} are taken as Gaussian random variables once certain physical constraints are imposed such as rotation invariance, time reversal invariance and conservation of total spin, isospin and parity.

As already mentioned, some analytical results for bosonic [5,9] and fermionic [3,4] models in the dilute limit were obtained, but here we consider the non-dilute limit, for which little is known. We want to find out how this limit and some other model dependencies, such as the nature of the particles or the system's

integrability, may affect the statistical properties of many-body systems.

Bosonic models

We study two bosonic models, the $U(4)$ vibron and $U(6)$ interacting boson models, used to explore molecular or nuclear collective excitations. In the $U(4)$ TBRE model, bosons with $J^\pi = 0^+(s, s^+)$ and $J^\pi = 1^-(\tilde{p}, p^+)$ are coupled to form a scalar Hamiltonian [10]

$$\begin{aligned} H_{U(4)} = & (\epsilon_s s^+ s + \epsilon_p p^+ \cdot \tilde{p}) / N_p \\ & + \left\{ \frac{c_0}{2} [p^+ p^+]^{(0)} \cdot [\tilde{p} \tilde{p}]^{(0)} \right. \\ & + \frac{c_2}{2} [p^+ p^+]^{(2)} \cdot [\tilde{p} \tilde{p}]^{(2)} \\ & + \frac{u_0}{2} [s^+ s^+]^{(0)} \cdot [s s]^{(0)} \\ & + \frac{u_1}{2} [s^+ p^+]^{(1)} \cdot [\tilde{s} \tilde{p}]^{(1)} \\ & \left. + \frac{v_0}{2\sqrt{2}} ([s^+ s^+]^{(0)} \cdot [\tilde{p} \tilde{p}]^{(0)} + \text{h.c.}) \right\} \\ & \times [N_p(N_p - 1)]^{-1}. \end{aligned} \quad (5)$$

The square brackets denote angular momentum coupling, the dots represent scalar products and N_p is the total number of bosons. Since the 1- and 2-body matrix elements are proportional to N_p and $N_p(N_p - 1)$, respectively, scaling allows all coefficients in (5) to be Gaussian random numbers of unit variance. For the choice of coefficients above, the lowest eigenvalue distribution has been obtained analytically, and in the large N_p limit [6]

$$\begin{aligned} P(E_{gs}) \propto & e^{-0.4E_{gs}^2} \text{erfc}(0.663E_{gs}) \\ & + 0.423e^{-0.467E_{gs}^2} \text{erfc}(0.632E_{gs}). \end{aligned} \quad (6)$$

The second model we investigate is the nuclear $U(6)$ model (IBM) which consists of scalar $J^\pi = 0^+(s, s^+)$ and quadrupole $J^\pi = 2^+(\tilde{d}, d^+)$ bosons coupled by one- and two-body interactions. The Hamiltonian has the form [11]

$$\begin{aligned} H_{U(6)} = & (\epsilon_s s^+ s + \epsilon_d d^+ \cdot \tilde{d}) / N_p \\ & + \left\{ \sum_{L=0,2,4} c_L [d^+ d^+]^{(L)} \cdot [\tilde{d} \tilde{d}]^{(L)} \right. \end{aligned}$$

$$\begin{aligned}
& + a_1 [s^+ d^+]^{(2)} \cdot [\tilde{d}\tilde{d}]^{(2)} \\
& + a_2 [s^+ s^+]^{(0)} \cdot [s s]^{(0)} \\
& + a_3 [s^+ d^+]^{(2)} \cdot [\tilde{s}\tilde{d}]^{(2)} \\
& + a_4 [s^+ s^+]^{(0)} \cdot [\tilde{d}\tilde{d}]^{(0)} + \text{h.c.} \left. \vphantom{a_1} \right\} \\
& \times [N_p(N_p - 1)]^{-1}. \tag{7}
\end{aligned}$$

We will consider $N_p = 16$, which is typical for a heavy collective nucleus, and the distribution for the ground state energy is obtained numerically. An important distinction between the $U(4)$ and $U(6)$ models is that the former is integrable for all parameters, while the latter is generally chaotic [12]. Chaos usually applies to fluctuation properties near the middle of the spectrum, rather than at the edges. Never the less, there is a subtle difference between these models which we attribute to the underlying chaos, as we discuss below. The ground states of these models also have well known phase transition behaviors. In spite of this, the ground state distributions will be seen to be surprisingly insensitive to this.

Fermionic models

The two fermionic models we investigate are a model for interacting nucleons in a single- j shell and a model for randomly interacting electrons. The single- j shell model consists of N_p identical fermions interacting with scalar, pairwise interactions $\mathcal{V}_{nn'}$ (for particles n and n') in a degenerate multiplet of spin j . We use $N_p = 6$ particles in the $j = 15/2$ shell. The Hamiltonian is in the form (4) with $\varepsilon_{ij} = 0$, since the interactions are two-body. Since the particles are identical, the sum over all pairwise interactions, $\sum_{n < n'} \mathcal{V}_{nn'}$, can be expressed in terms of a single two-body matrix element

$$v_{J'} = \langle j^2(J')J | \mathcal{V}_{nn'} | j^2(J')J \rangle$$

using coefficients of fractional parentage [13]. Note that the particle indices drop from the equation. Consequently, there is a large reduction in the number of distinct matrix elements, and the Hamiltonian (4)

reduces to [13]

$$\begin{aligned}
& \langle j^{N_p} \alpha J M | \sum_{n < n'}^{N_p} \mathcal{V}_{nn'} | j^{N_p} \alpha' J M \rangle \\
& = \frac{N_p(N_p - 1)}{2} \\
& \times \sum_{\alpha'', J'', J'} [j^{N_p} \alpha J \{ | j^{N_p-2}(\alpha'' J'') j^2(J') J \} \\
& \quad \times [j^{N_p-2}(\alpha'' J'') j^2(J') J \} \\
& \quad \times j^{N_p} \alpha' J \} v_{J'}]. \tag{8}
\end{aligned}$$

Here J is the total angular momentum, M is the z -projection, α denotes all other quantum numbers, the term in brackets corresponds to the coefficients of fractional parentage. The matrix elements $v_{J'}$ ($J' = 0, 2, \dots, 2j - 1$) are Gaussian random numbers.

The second fermionic model is a model for randomly interacting $j = 1/2$ fermions (IEM) and is given by [15]

$$H = \sum_{\alpha j} \epsilon_{\alpha} a_{\alpha j}^{\dagger} a_{\alpha j} + \sum_{\alpha \beta \gamma \eta j j'} U_{\alpha \beta}^{\gamma \eta} a_{\alpha j}^{\dagger} a_{\beta j'}^{\dagger} a_{\gamma j} a_{\eta j}, \tag{9}$$

where the one-body spectrum is Wigner–Dyson distributed with $\epsilon_{\alpha} \in [-K/2; K/2]$ ($K/2$ gives the number of spin-degenerate orbitals, the average level spacing is then $\Delta = 1$), $U_{\alpha \beta}^{\gamma \eta} \in [-U; U]$ are Gaussian random numbers and $j(j') = \uparrow(\downarrow)$ are spin indices. We study up to $N_p = 7$ fermions on $K/2 = 7$ orbitals.

While the single j -shell model describes non-chaotic system [14], the spectral properties of the IEM depend on the ratio of the interaction strength to the one-body level spacing U/Δ : for $U/\Delta \ll 1/(KN_p^2)$ the model is non-chaotic with a Poissonian spectrum while for $U/\Delta \gg 1/(KN_p^2)$ it is chaotic with a Wigner–Dyson distributed spectrum [16].

To compare the lowest eigenvalue distribution for these four models with the ones for the GOE, we re-center the distributions and rescale their widths by using the following scaling prescription

$$\varepsilon_{\text{gs}} = \frac{E_{\text{gs}} - \langle E_{\text{gs}} \rangle}{\sigma_{E_{\text{gs}}}}. \tag{10}$$

This removes model dependencies associated with scales, level densities and so forth. We show in Fig. 2 distributions of the rescaled ground state energy ε_{gs} for

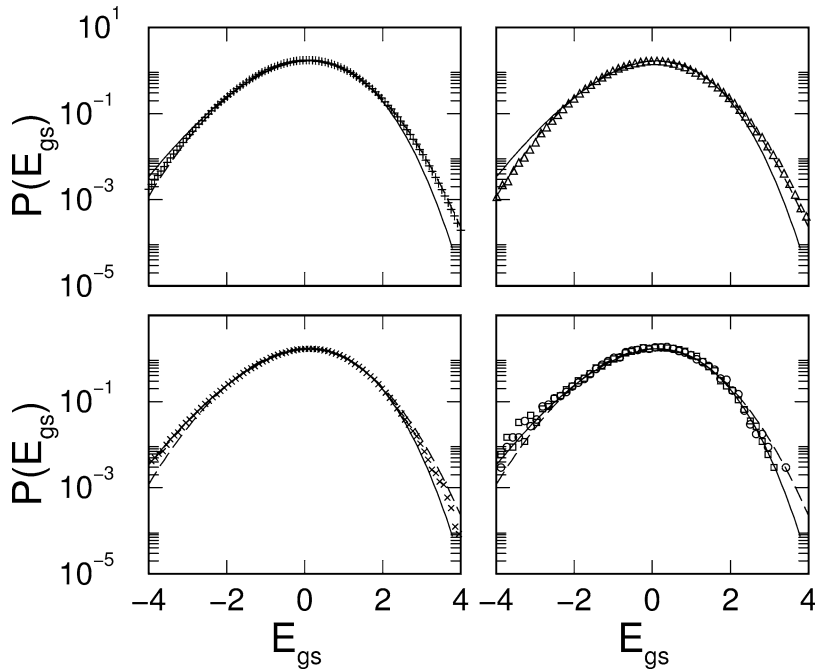


Fig. 2. Distributions of the ground state energy for the vibron model (top left), the single j -shell model (top right), the IBM (bottom left) and the IEM (bottom right) for $N_p = 3$ (circles) and 4 (squares). In all panels, dashed and solid lines give the distribution for the $N = 2$ and $N = \infty$ GOE, respectively. The top panels correspond to non-chaotic systems, for which the data are well fitted by a $N = 2$ GOE. The bottom panels correspond to chaotic systems, where data are closer to the $N = \infty$ GOE.

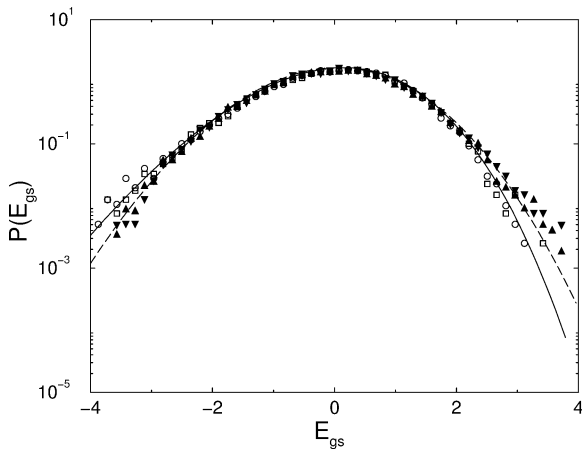


Fig. 3. Crossover to quantum chaos for the IEM with $N_p = 4$ and $U/\Delta = 10^{-7}$ (diamonds), 0.05 (triangles), 1 (squares) and ∞ (circles). Symbols for data in the integrable regime are filled, while dashed and solid lines give the distribution for the $N = 2$ and $N = \infty$ GOE, respectively.

the four models described above. The figure splits into regular systems on the top two panels and chaotic ones on the two bottom panels. Bosonic models are left and fermionic ones are right. The chaoticity of the IEM depends on U/Δ and the data shown on the lower right panel of Fig. 2 for the IEM correspond to $U/\Delta = 1$, well into the chaotic regime [16].

One clearly sees that the ground state energies have approximately the same distribution for the four TBREs and the GOE of small and large dimension—this seems to be a robust property, and in particular, these distributions seem not to depend on the nature of the particles. Moreover, the agreement of the distributions with the ones obtained from the GOE demonstrates that the distribution of the ground state energy is also not sensitive to the type of ensemble used. A closer inspection of the presented data does reveal discrepancies between different models in the distribution tails. The lowest energy distribution for regular systems coincides better with the distribution for the two-dimensional GOE, while the distribution

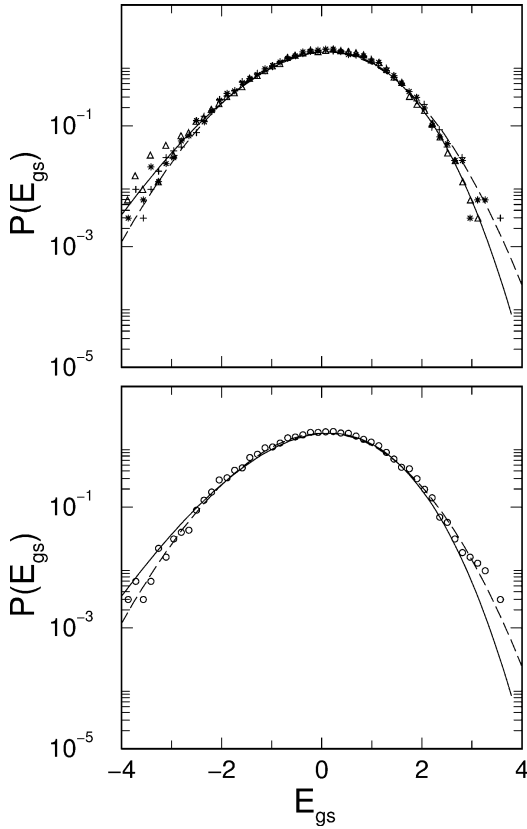


Fig. 4. Top panel: distribution of the ground state energy for the IEM for $N_p = 4$ (triangles), 5 (crosses) and 6 (stars). Bottom panel: distribution of the ground state energy for the IEM at half filling, $N_p = 7$ (circles). In both panels, dashed and solid lines give the distribution for the $N = 2$ and $N = \infty$ GOE, respectively. The particle statistics plays a role at half-filling only, rendering the distribution closer to the $N = 2$ GOE.

for chaotic systems is in better agreement with the one obtained with a large- N GOE. The GOE dimension necessary to describe a system can be associated with the integrability of the model. This conclusion is corroborated by the data shown on Fig. 3 for the IEM at various U/Δ , both in the integrable and chaotic regimes. Evidently the crossover from Poisson to Wigner–Dyson distributed level spacing (i.e., from integrable to chaotic quantum dynamics) is accompanied by a crossover from two-dimensional to infinite-dimensional GOE fitting of the ground-state distribution. We also found that the ground-state distribution for the IEM exactly at half-filling ($K = 14$ and $N_p = 7$), gets close to a two-dimensional

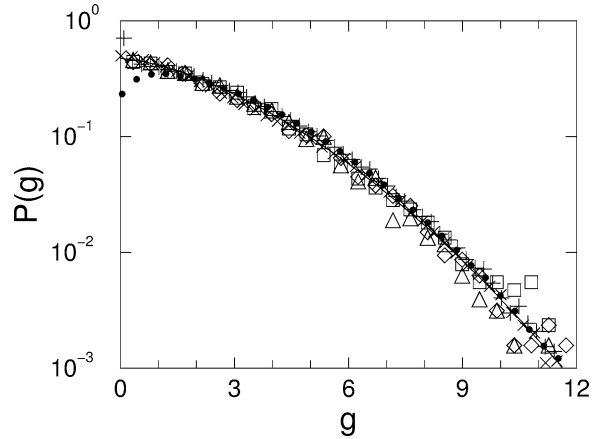


Fig. 5. Spin gap distribution for the $U(4)$ vibron model (\times) the $U(6)$ IBM ($+$) the single j -shell model (\bullet) and the IEM with $N_p = 5$ (triangles), 6 (squares) and 7 (diamonds). The solid line corresponds to the analytical expression obtained for the vibron model. The only significant deviations occur for the single j -shell model for low gap values.

GOE, as shown at the top of Fig. 4. Since the associated spectrum is still Wigner–Dyson distributed, we conclude that this is a manifestation of the particle statistics. The only influence of the latter therefore is to single out half-filled fermionic systems which despite their chaotic character have a distribution of ground-state energies which is closer to the $N = 2$ GOE.

Consider now distributions which cannot be addressed through RMT, namely distributions which involve correlations between Hilbert subspaces with different quantum numbers. One quantity of fundamental interest is the energy gap. In the models we study, this typically involves states of different spin: for the vibron model it is

$$\varepsilon(J^\pi = 1^-) - \varepsilon(J^\pi = 0^+),$$

for the IBM

$$\varepsilon(J^\pi = 2^+) - \varepsilon(J^\pi = 0^+),$$

while for the single j -shell model and the IEM

$$\varepsilon(J = 1) - \varepsilon(J = 0).$$

We will call this energy difference the *spin gap*. The ground state is mostly dominated by 0^+ (this predominance almost reaches 100% for the IEM [15]) and the lowest level with a different spin usually corresponding to the first excited state (this is however

not the case for the IEM), so we are looking at the very edge of the spectrum. Even though we have both bosonic and fermionic models, the distributions are very similar and also agree very well with the analytical expression derived for the vibron model [6] as it is evident from Fig. 5. The distribution of the spin gaps is thus also a generic property which we attribute to the bosonic nature (i.e., δJ is an integer) of the corresponding excitation in all four models studied here. This explains why the particle statistics have no influence here. Note that in the case of the IEM, universality of the spin gap requires a finite interaction strength $U/\Delta \gtrsim 1$. In the limit $U/\Delta \rightarrow 0$, the spin gap is determined by the one-body spectrum ϵ_α and thus given by a GOE one- (two-) spacing distribution for N_p even (odd).

In summary, investigating various TBREs, we have found that in spite of their fundamental differences, they have strikingly similar features in both their ground state energy distribution and their spin gap distribution. The ground state energy distributions have common features, and coincide to GOE distributions of either small or large dimensions, for regular or chaotic TBREs, respectively. We conclude that the edge of the spectra exhibit two unexpected generic properties: the distribution of the ground state energy and the distribution of the energy differences between the lowest levels with different spins. This latter point is presumably related to the apparent regular structure found in the angular momentum structure of low-lying levels for several TBREs [17].

Acknowledgements

L.F. Santos acknowledges the support of the Fundação de Amparo à Pesquisa do Estado de São Paulo

(FAPESP) and Ph. Jacquod has been supported by the Swiss National Science Foundation.

References

- [1] E.P. Wigner, *Ann. Math.* 53 (1951) 36.
- [2] T. Guhr, A. Müller-Groeling, H.A. Weidenmüller, *Phys. Rep.* 299 (1998) 190.
- [3] T.A. Brody, J. Flores, J.B. French, P.A. Mello, A. Pandey, S.S.M. Wong, *Rev. Mod. Phys.* 53 (1981) 385.
- [4] J.B. French, S.S.M. Wong, *Phys. Lett. B* 33 (1970) 449; O. Bohigas, J. Flores, *Phys. Lett. B* 34 (1971) 261.
- [5] V.K.B. Kota, V. Potbhare, *Phys. Rev. C* 21 (1980) 2637.
- [6] D. Kusnezov, *Phys. Rev. Lett.* 85 (2000) 3773.
- [7] C.A. Tracy, H. Widom, *Commun. Math. Phys.* 177 (1996) 727.
- [8] Ya.G. Sinai, A.B. Soshnikov, *Func. Anal. Appl.* 32 (1998) 114.
- [9] V.R. Manfredi, *Nuovo Cimento A* 64 (1981) 101; P.F. Bortignon, V.R. Manfredi, *Lett. Nuovo Cimento* 23 (1978) 219; P.F. Bortignon, M. Dalla Francesca, V.R. Manfredi, *Lett. Nuovo Cimento* 19 (1977) 15.
- [10] F. Iachello, R.D. Levine, *Algebraic Theory of Molecules*, Oxford Univ. Press, New York, 1995.
- [11] A. Arima, F. Iachello, *The Interacting Boson Model*, Cambridge Univ. Press, Cambridge, 1987.
- [12] Y. Alhassid, N. Whelan, *Phys. Rev. Lett.* 67 (1991) 816.
- [13] A. deShalit, I. Talmi, *Nuclear Shell Theory*, Academic Press, New York, 1963.
- [14] V. Zelevinsky, B.A. Brown, N. Frazier, M. Horoi, *Phys. Rep.* 276 (1996) 85.
- [15] Ph. Jacquod, A.D. Stone, *Phys. Rev. Lett.* 84 (2000) 3938; L. Kaplan, T. Papenbrock, *Phys. Rev. Lett.* 84 (2000) 4553.
- [16] Ph. Jacquod, D.L. Shepelyansky, *Phys. Rev. Lett.* 79 (1997) 1837.
- [17] C.W. Johnson, G.F. Bertsch, D.J. Dean, *Phys. Rev. Lett.* 80 (1998) 2749; R. Bijker, A. Frank, S. Pittel, *Phys. Rev. C* 60 (1999) 021302; S. Drozd, M. Wójcik, *nucl-th/0007045*; Ph. Jacquod, A.D. Stone, *Phys. Rev. B* 64 (2001) 214416; V.K.B. Kota, K. Kar, to appear in *Phys. Rev. E*.